Impact of land use on Costa Rican tropical montane cloud forests: Sensitivity of cumulus cloud field characteristics to lowland deforestation

U. S. Nair,[1] R. O. Lawton,[2] R. M. Welch,[1] and R. A. Pielke Sr.[3]

Received 23 July 2001; revised 24 October 2002; accepted 24 October 2002; published 3 April 2003.

[1] Recent studies have shown that there has been a reduction in dry season moisture input from direct interception of cloud water and wind-blown mist at the lee edge of the Monteverde cloud forest, Costa Rica, since the mid 1970s. This reduction of moisture could be responsible for the population crashes of anurans observed in the region. It has been hypothesized that this behavior is a result of increases in cloud base height, linked to increased sea surface temperatures. In this study we present a complementary hypothesis, that deforestation upwind of the Monteverde cloud forest preserve is responsible for the observed changes in cloud base height. An automated cumulus cloud classification scheme extracts monthly spatial maps of the frequency of occurrence of cumulus cloudiness over Costa Rica from GOES 8 visible channel satellite imagery. We find that cumulus cloud formation in the morning hours over deforested regions is suppressed compared to forested areas. The degree of suppression appears to be related to the extent of deforestation. This difference in cloud formation between forested and deforested areas is a clear signal of land use change influencing the regional climate. Regional Atmospheric Modeling System numerical modeling simulations are used to explore the differences in cloud field characteristics over the lowland pasture and forest landscapes. Statistically significant differences in cloud base height and cloud thickness occur between the forest and pasture simulations. Clouds have higher base heights and are thinner over pasture landscapes than over forested ones. On the other hand, these simulations show no statistically significant differences in cloud top heights, cloud cover, mean cloud water mixing ratio, or cloud liquid water path between pasture and forest simulations. However, in the simulations there are enhanced sensible heat fluxes and reduced latent heat fluxes over pasture compared to forest. It is the drier and warmer air over pasture surfaces that results in the formation of elevated thinner clouds. This study suggests that deforestation results in warmer, drier air upwind of the Monteverde cloud forests and that this could influence the base height of orographic cloudbanks crucial to the region during the dry season. *INDEX TERMS:* 0322 Atmospheric Composition and Structure: Constituent sources and sinks; 3314 Meteorology and Atmospheric Dynamics: Convective processes; 0315 Atmospheric Composition and Structure: Biosphere/atmosphere interactions; 1803 Hydrology: Anthropogenic effects; *KEYWORDS:* tropical montane cloud forests, deforestation, cumulus clouds, cloud base height, mesoscale modeling, climatic influence of land use

Citation: Nair, U. S., R. O. Lawton, R. M. Welch, and R. A. Pielke Sr., Impact of land use on Costa Rican tropical montane cloud forests: Sensitivity of cumulus cloud field characteristics to lowland deforestation, *J. Geophys. Res.*, *108*(D7), 4206, doi:10.1029/2001JD001135, 2003.

1. Introduction

[2] Tropical montane cloud forests (TMCFs) depend upon predictable, frequent and prolonged immersion in cloud [*Bruinjzeel and Proctor*, 1995; *Pounds et al.*, 1999]. In the Cordillera de Tilarán of Costa Rica, anuran population crashes, increases in the upper elevation of bird ranges on the Pacific slope, and longer mist-free intervals in the dry season at the lee edge of the Monteverde TMCF have been attributed to an increase in the base height of the orographic cloudbank due to changes in sea surface temperature [*Pounds et al.*, 1999; *Still et al.*, 1999]. This study proposes a complementary hypothesis: that upwind lowland deforestation alters surface energy budgets in ways that reduce the development of tropical dry season cumulus cloud fields and raise cloud base heights. In this paper corroborating evidence is offered from remote sensing of clouds in

[1]Department of Atmospheric Science, National Space Science and Technology Center, University of Alabama in Huntsville, Huntsville, Alabama, USA.
[2]Department of Biological Sciences, University of Alabama in Huntsville, Huntsville, Alabama, USA.
[3]Department of Atmospheric Science, Colorado State University, Fort Collins, Colorado, USA.

0148-0227/03/2001JD001135$09.00

northern Costa Rica and southern Nicaragua, and from regional atmospheric simulations of idealized simple lowland tropical forest and pasture landscapes. Since TMCFs are crucial components of most tropical biodiversity "hotspots," and play important roles in local and regional hydrological management, factors that influence TMCF distribution and water budget are a matter of considerable interest.

[3] In the Caribbean basin, as in much of the tropics, TMCFs occur where mountains force trade winds to rise past the point at which adiabatic cooling results in cloud formation. In such settings, upwind regional landscape characteristics can influence the overlying atmosphere in ways that may have important consequences for cloud formation, and consequently for TMCFs.

[4] It has been long recognized that through modulation of surface energy budgets, land use can have significant influence on the regional climate. Land use changes are usually accompanied by variations in surface properties such as albedo, temperature, roughness length, water storage capacity of surface soil and soil moisture distribution [*Otterman*, 1974; *Sagan et al.*, 1979; *Anthes*, 1984; *Segal et al.*, 1988; *Shukla et al.*, 1990; *Meher-Homji*, 1991; *Gash and Nobre*, 1997; *Pielke*, 2001]. Variations in surface properties also can cause changes in boundary layer air temperature, moisture, and depth, as well as local rainfall and cloudiness [*Segal et al.*, 1988; *Bryant et al.*, 1990; *Otterman et al.*, 1990; *Schwartz and Karl*, 1990; *Meher-Homji*, 1991; *Bastable et al.*, 1993; *Sud et al.*, 1993; *Lyons et al.*, 1993; *Gash and Nobre*, 1997; *Pielke*, 2001].

[5] Cumulus clouds are strongly influenced by the surface, since they form from thermals induced in the boundary layer. For example, the suppression of cumulus cloudiness over water bodies has been observed since the early days of satellite imagery [*Segal et al.*, 1997]. In addition satellite imagery has shown preferential formation of cumulus clouds over areas with relatively higher sensible heat fluxes such as harvested wheat fields and deforested regions [*Rabin et al.*, 1990; *Lyons et al.*, 1993; *Cutrim et al.*, 1995; *Rabin and Martin*, 1996]. On the other hand, increased soil moisture caused by irrigation can enhance the convective available potential energy (CAPE), thereby increasing the probability of sustained convection [*Pielke and Zeng*, 1989]. The influence of land surface on cumulus cloud formation also is dependent on the stability of the overlying atmosphere. Under stable atmospheric conditions, clouds may develop earlier over moist surfaces, while for weakly stable conditions, clouds form earlier over drier surfaces [*Wetzel et al.*, 1996]. Land surface heterogeneity also can have a significant influence on the formation and development of the convective clouds. The majority of the modeling and theoretical studies show that differential heating over contrasting surfaces results in the generation of mesoscale circulations that enhance cloudiness [*Anthes*, 1984; *Ookouchi et al.*, 1984; *Segal et al.*, 1988; *Chen and Avissar*, 1994; *Avissar and Liu*, 1996; *Emori*, 1998; *Avissar and Schmidt*, 1998]. Indeed, *Avissar and Liu* [1996] note that updrafts produced by surface heterogeneity are usually stronger than those resulting from turbulence. Over regions where convective rainfall creates a heterogeneous soil moisture distribution, *Emori* [1998] found that convergence of air over drier soil initiates convective clouds. The rain from these convective clouds makes the soil wetter than the surroundings, thereby maintaining the heterogeneity of the soil moisture distribution. *Pielke* [2001] provides a detailed review on the influence of vegetation, soil properties, surface heterogeneity on cumulus cloudiness and rainfall.

[6] The Costa Rican lowlands are an environmentally complex region in which the original tropical forests are being rapidly replaced by pastures and agricultural landscapes. *Sader and Joyce* [1988] estimate that the primary forest in Costa Rica decreased from 67% in 1940 to 17% in 1983. Land use changes in the Caribbean lowlands can alter the nature of the air masses responsible for the formation of cumulus clouds in the lowlands as well as orographic clouds on the Caribbean slopes. In view of the large-scale deforestation in the Caribbean lowland region east of Monteverde and the significant influence it may exert on cloud formation, land use changes cannot be ruled out as a causative factor for the observed climate change in the Monteverde region. In this study the effects of lowland deforestation on cumulus cloud formation and development are examined using satellite data and a mesoscale numerical model.

[7] The two main objectives of this study are to: (1) use Geostationary Operational Environmental Satellite 8 (GOES 8) and LANDSAT Multi-Spectral Scanner (MSS) imagery to examine the effect of deforestation on cloud formation, and (2) use the Regional Atmospheric Modeling System (RAMS), a mesoscale numerical model, to investigate the effects of deforestation on cloud characteristics, especially cloud base heights.

[8] Section 2 describes the data, and section 3 discusses the methodology used in this study. The results from both the analysis of satellite data and RAMS simulations are presented in section 4, and section 5 concludes.

2. Data

[9] GOES 8 imagery has 5 spectral channels, one in the visible (0.52–0.72 μm) and four in the infrared region (3.78–4.03 μm, 6.47–7.02 μm, 10.2–11.2 μm, 11.5–12.5 μm). Spatial resolution at nadir for channel 1 is 1 km, 4 km for channels 2, 4, and 5, and channel 3 has nadir resolution of 8 km. The visible channel is used for the mapping of cumulus clouds in the present study. Daytime GOES 8 imagery over the Central American region is taken at 2 hour temporal resolution for the months of February, March and April 1999. The GOES 8 visible channel data are calibrated and normalized by the cosine of solar zenith angle to yield the albedo values. Landsat Multi Spectral Scanner (MSS), used in this study to investigate deforestation and cloudiness patterns, has four spectral bands in the range 0.5 to 0.6 μm, 0.6 to 0.7 μm, 0.7 to 0.8 μm, and 0.8 to 1.1 μm with spatial resolution of 57 m nadir.

[10] Radiosonde profiles from the coastal plains of Costa Rica would be ideal for simulating the development of lowland cumulus cloud fields, but are not available, so we use six 1200 UTC (0600 LST) soundings from San Andres island (to the east, and upwind of Costa Rica). These soundings are chosen for days characterized by relatively calm synoptic conditions and by the observed presence of

Table 1. The Date of Acquisition and Characteristics of the Six 1200 UTC Radiosonde Observations, From San Andres Island in the Carribbean, Used in This Study[a]

Sounding	Date	CAPE, J/kg	CIN, J/kg	LCL, m
S1	3/01/1999	576	1	506
S2	3/03/1999	680	3	537
S3	3/11/1999	971	1	523
S4	3/19/1999	248	1	605
S5	3/24/1999	947	1	565
S6	3/27/1999	1404	1	411

[a]The sounding characteristics listed are Convective Available Potential Energy (CAPE), Convective Inhibition (CIN), Lifting Condensation Level (LCL) and Level of Free Convection (LFC).

fair weather cumulus clouds in Costa Rica. The convective available potential energy (CAPE), convective inhibition (CIN), and lifting condensation level (LCL) associated with these soundings are given in Table 1. The values of CAPE, which vary between 248–1404 Jkg^{-1}, are indicative of weak to moderate convection [*Bluestein*, 1992] and are thus suitable for formation of fair weather cumulus. The low CIN values (1–3 Jkg^{-1}) imply an environment where convection can be easily initiated. Lifting condensation level values, which provide an estimate of cloud base during early hours of cloud formation, are within the range of cloud base heights estimated from Landsat data (see below).

3. Methodology

3.1. Analysis of Satellite Data

[11] The frequency of occurrence of cumulus cloudiness in Costa Rica for the dry season months of February, March and April, 1999, is derived from GOES 8 visible imagery using structural thresholding, an automated cumulus cloud detection algorithm [*Nair et al.*, 1999; *Nair*, 2002]. The structural thresholding approach uses the spatial structure of the cloud elements within a cloud field to determine the extent of cumulus cloud fields as well as to detect individual clouds within a scene. Once the cumulus cloud fields are identified, the cloud elements within the cloud fields are labeled as cumulus clouds. *Nair* [2002] compared the performance of a variety of cumulus cloud field detection algorithms and determined that the structural thresholding approach was the most accurate, providing a classification accuracy of 87% for cumulus cloud fields and 89% accuracy for identifying correctly the cumulus clouds within the fields.

[12] The structural thresholding algorithm is used to derive the cumulus cloud mask for the Caribbean region of Costa Rica daily at 1415 UTC (0815 LST, UTC = LST + 6 hrs), 1615 UTC, 1815 UTC and 2015 UTC for the ecologically critical dry season months of February, March and April, 1999. The influence of surface characteristics on cloud formation is likely to be most significant during the dry season, due to relatively calmer synoptic situations at this time. Further, the surface fluxes in both forested and deforested regions are expected to be higher in the dry season. Monthly maps of frequency of occurrence of cumulus clouds for 1415 UTC, 1615 UTC, 1815 UTC and 2015 UTC over the Costa Rican region are derived from the daily cumulus cloud masks. Frequency of cumulus cloud occurrence is expressed as percentage of observations in a month for which cumulus clouds are present over a particular location.

3.2. Numerical Modeling Experiments

[13] The RAMS model is nonhydrostatic and is used for the simulation of atmospheric phenomenon ranging from cloud scale to mesoscale [*Pielke et al.*, 1992]. RAMS uses finite difference methods for solving the various conservation equations governing the atmospheric flow. Cloud microphysics is represented in RAMS using bulk water parameterization which includes cloud water, rain, pristine ice, snow aggregates, graupel and hail categories. At the lower boundary, RAMS uses a multilayer soil model [*Tremback and Kessler*, 1985] and a vegetation model [*Avissar and Pielke*, 1989] to represent the land surface processes. Various options are available for representation of radiative transfer, turbulence and lateral boundary conditions.

[14] The effect of varied surface conditions on cloud formation was examined using a coupled design in which each of six sounding (S1–S6) was used for initialization of both forest and pasture atmospheric conditions. The impact of deforestation and conversion to pasture was examined by comparing diurnally developing conditions between simulations. It was assumed that the vegetation in the forest simulations had transfer characteristics of evergreen broadleaf forest, with initial volumetric soil moisture set to 0.4, while pasture simulations had transfer characteristics of short grass, with initial volumetric soil moisture set to 0.25. These forest volumetric soil moisture values are appropriate to tropical evergreen forest dry season values for the region [*Dietrich et al.*, 1982], and the pasture volumetric soil moisture yields results consistent with empirical micrometeorological studies over Amazonian pasture [*Bastable et al.*, 1993; *Wright et al.*, 1992].

[15] The cloud field simulations were performed over a domain of 100 km × 100 km represented by 100 × 100 horizontal grid points at uniform horizontal grid spacing of 1 km. In the vertical, a stretched grid with a stretch ratio of 1.08 was used, providing vertical spacing ranging from 70 m near the surface to a maximum of 750 m higher up in the atmosphere. The terrain adopted in these model simulations was flat. A periodic boundary condition was assumed at the lateral boundaries, and a rigid top boundary was adopted. Of the different radiative transfer schemes available for the RAMS, the *Chen and Cotton* [1983] radiative transfer scheme was used to account for the effect of clouds. The anisotropic deformation scheme was used to represent horizontal and vertical diffusion processes. Cloud formation processes other than those involving ice processes were activated. Precipitation processes were not activated in these simulations to save computer-processing resources since the cloud fields simulated were almost exclusively fair weather cumulus.

[16] For each of the six soundings (S1–S6), the model was integrated with forest and pasture surface conditions for 12 hours starting at 1200 UTC, approximately local dawn. The simulations with atmospheric conditions represented by soundings S1 through S6 and forest surface conditions are referred as F1, F2, F3, F4, F5 and F6. Similarly the coupled simulations with pasture surface conditions are referred to as P1, P2, P3, P4, P5 and P6. For each simulation the initial atmospheric conditions were set to be horizontally homo-

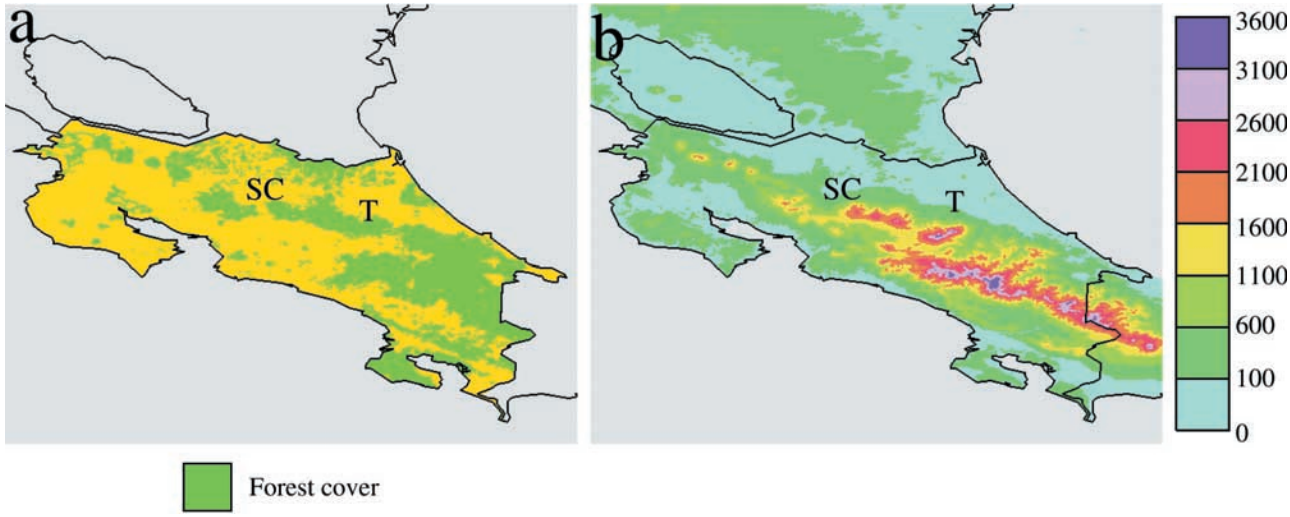

Figure 1. (a) Recent estimates of forest cover in Costa Rican region. (b) Topography of the Costa Rican region in meters. The labeled areas in the images are San Carlos plains (SC) and Tortuguero plains (T).

genous with the vertical structure prescribed by each atmospheric sounding.

[17] The diurnal variations of domain averaged cloud base height, cloud top height, cloud thickness, cloud cover, cloud water mixing ratio, liquid water path, sensible heat flux, latent heat flux, surface temperature and surface dewpoint temperature from simulations F1–F6 are compared to those from corresponding simulations P1–P6. Vertical columns with integrated liquid water path greater than or equal to 0.2 kg m-2 were assumed to contain cumulus cloud. Within each column containing cumulus cloud, cloud base height was assumed to be the height of grid point with non-zero liquid water content closest to the surface. The cloud top height is chosen as the height of the topmost grid point of a run of consecutive non-zero liquid water content grid points, starting from the cloud base grid point.

4. Results

[18] The satellite analysis covers the dry season months of February through April 1999 in which the data has been processed at 1615, 1815 and 2015 UTC (1015, 1215, and 1415 LST). Deforested regions have a lower incidence of cumulus clouds and the clouds that do form in these regions are smaller than those in nearby forested regions. The numerical modeling simulations examine the diurnal development of cumulus clouds above both pastures and forests. In the simulations clouds in forested regions have lower base heights than those those in pastured landscapes. Since most tropical montane cloud forests lie downwind of lowland areas, this raises serious conservation concerns at sites like the Monteverde cloud forests of the Cordillera de Tilarán.

4.1. GOES 8 Satellite Imagery Analysis

[19] Interpretation of the GOES 8 imagery requires a brief consideration of the geography of northern Costa Rica and southern Nicaragua (Figure 1b). The Cordillera de Tilarán runs as a single sinuous central ridge (the continental divide) about 70 km from the western margin of Costa Rica's Meseta Central to the southeastern tip of the chain of isolated volcanoes which extends into Nicaragua. The Cordillera rises abruptly from the Pacific coast, reaching peaks of about 1800 m elevation 25 km inland. The northeast trade wind flow in the region is such that the Cordillera de Tilarán is downwind of the Nicaraguan/Costa Rican Caribbean coastal plain.

[20] Deforestation and agricultural conversion in Costa Rica has been rapid (estimated at 400–600 km^2/yr in the late 70s and early 80s) [*Sader and Joyce*, 1988], with the result that less than 1,000 km^2 of undisturbed forest remained on the Costa Rican portion of the coastal plain in 1993 (J. Mendez, personal communication, 1992). There have been no major deforestation activities since the mid-1980s in the Costa Rican coastal plains, but rather a gradual erosion of the forested regions at the boundaries [*Wheelwright*, 2000] (Figures 1a and 2a). In contrast, political conflicts have hindered agricultural development in adjacent Nicaragua, with the result that the original forest there is much more intact (Figures 1a, 2a, and 2b). Landsat imagery often shows that dry season cumulus clouds do not form in the San Carlos and Tortuguero plains, which have long been deforested and converted to pasture and cropland [*Sader and Joyce*, 1988; *Wheelwright*, 2000] (Figure 2a). When cumulus clouds do form in these regions, as in Figure 2b, the clouds generally are smaller and less well developed than clouds just north of the border in the forested Nicaraguan lowlands.

[21] Figure 3 shows the percent frequencies of occurrence of total cloud cover and cumulus cloud cover over southern Nicaragua and Costa Rica retrieved at 1615, 1815 and 2015 UTC for March, 1999, using the method described in section 3. Extensive cumulus cloud cover (Figure 3, right panels) is found along the Mosquito Coast (in NE Nicaragua, not shown) and extending down to the border with Costa Rica. These regions are predominately forested. Note the rather abrupt decrease in cumulus cloud cover near the Nicaragua-Costa Rica border. The highest frequency of occurrence of cumulus cloudiness occurs at 1615 UTC

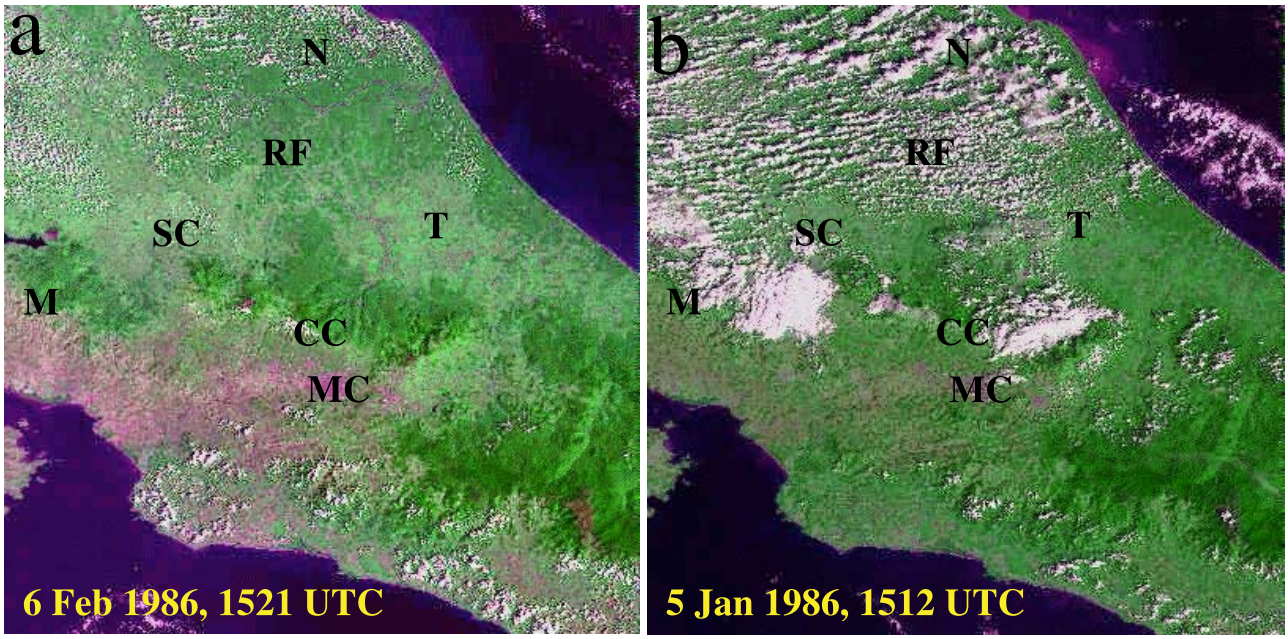

Figure 2. Deforestation and dry season cumulus cloud cover in northern Costa Rica and southern Nicaragua. False color Landsat images over Costa Rica for (a) 6 February 1986 at 1521 UTC and (b) 5 January 1986 at 1512 UTC. The labeled areas in the images are San Carlos plains (SC), Tortuguero plains (T), Monteverde (M), Cordillera Volcanica Central (CC), deforested lee in the Meseta Central (MC), Remnant forest (RF) south of the Costa Rica-Nicaragua border and intact lowland forest covers southeastern Nicaragua (N). The color composite is created by combining red, green and blue intensities in proportion to brightness values for band 2, 4 and 1.

and then decreases throughout the day. This behavior is due to the fact that moisture is available in the morning hours to initiate cumulus cloud formation. Heating then dries out the boundary layer so that cumulus cloudiness decreases later in the day. Figure 3 (left panels) shows total cloudiness. In southern Nicaragua total cloud cover is maximum about local noon (1815 UTC) and then decreases. Heating causes strong convection so that larger clouds form at this time. However, the drying of the atmosphere once again leads to a lower cloud cover later in the day.

[22] Dry season cumulus cloudiness in northern Costa Rica is much lower than in neighboring Nicaragua (Figure 3). Furthermore, the cumulus cloudiness is associated with the presence of forests, as seen by comparing Figures 1, 2, and 3. Dry season cumulus cloudiness is maximum in the Caribbean lowlands of Costa Rica at about local noon (1815 UTC) and then decreases rapidly. Of particular interest are the two extensively deforested patches (denoted as SC and T in the LANDSAT image, Figure 2) to the east of the Monteverde cloud forests in the Cordillera de Tilarán. The region T is closer to the ocean and has a higher frequency of occurrence of cumulus clouds. As seen on the LANDSAT imagery (Figure 2), cumulus clouds in the deforested regions generally have smaller diameters. The frequency of occurrence of cumulus clouds is higher over forested regions, except over forested mountain, where orographic clouds dominate. On the other hand, total cloud cover in Costa Rica is strongly correlated with topography, as seen by comparing Figure 3 with Figure 1b. Regions of rapid elevation change cause uplifting which is conducive to total cloudiness but not cumulus cloud development. The maximum dry season total cloud cover occurs at about noon (1815 UTC).

[23] Cumulus cloud fields in the dry season months of February and April are very similar to those in March (data not shown). On the other hand, total cloudiness is larger in both February and April than in March, especially in southern Nicaragua and along the Cordillera de Tilarán. In both February and April, total cloud cover is maximum at 2015 UTC in the Cordillera de Tilarán.

[24] The lack of cloud cover over Lake Nicaragua is typical of the cloud clearing that is observed over lakes, bays and wide rivers (Figure 3) [*Gibson and Vonder Haar*, 1990; *Rabin et al.*, 1990]. The area affected is larger than the actual size of the lake, especially in the downwind (left side of the image) direction. This behavior is similar to the flow divergence field downwind of Lake Okeechobee observed by *Pielke* [1974]. *Segal et al.* [1997] suggested that drying by dynamically induced subsidence and suppression of the convective boundary layer over lakes contribute to the cloud clearing. One other interesting feature is that both the Atlantic and Pacific oceans are nearly free of cumulus cloud fields during all three months. Total cloud cover over the Caribbean and Pacific oceans is significantly higher in both February and April than in March.

[25] These results for 1999 cloud cover appear representative of the region. Similar maps of cumulus and total cloudiness, developed for February through April 2000 and for February 2001, show that while there are variations over specific locations, the overall pattern is consistent with the results for 1999. In 2000 the cover by dry season cumulus cloud fields was a little higher over Nicaragua for all three

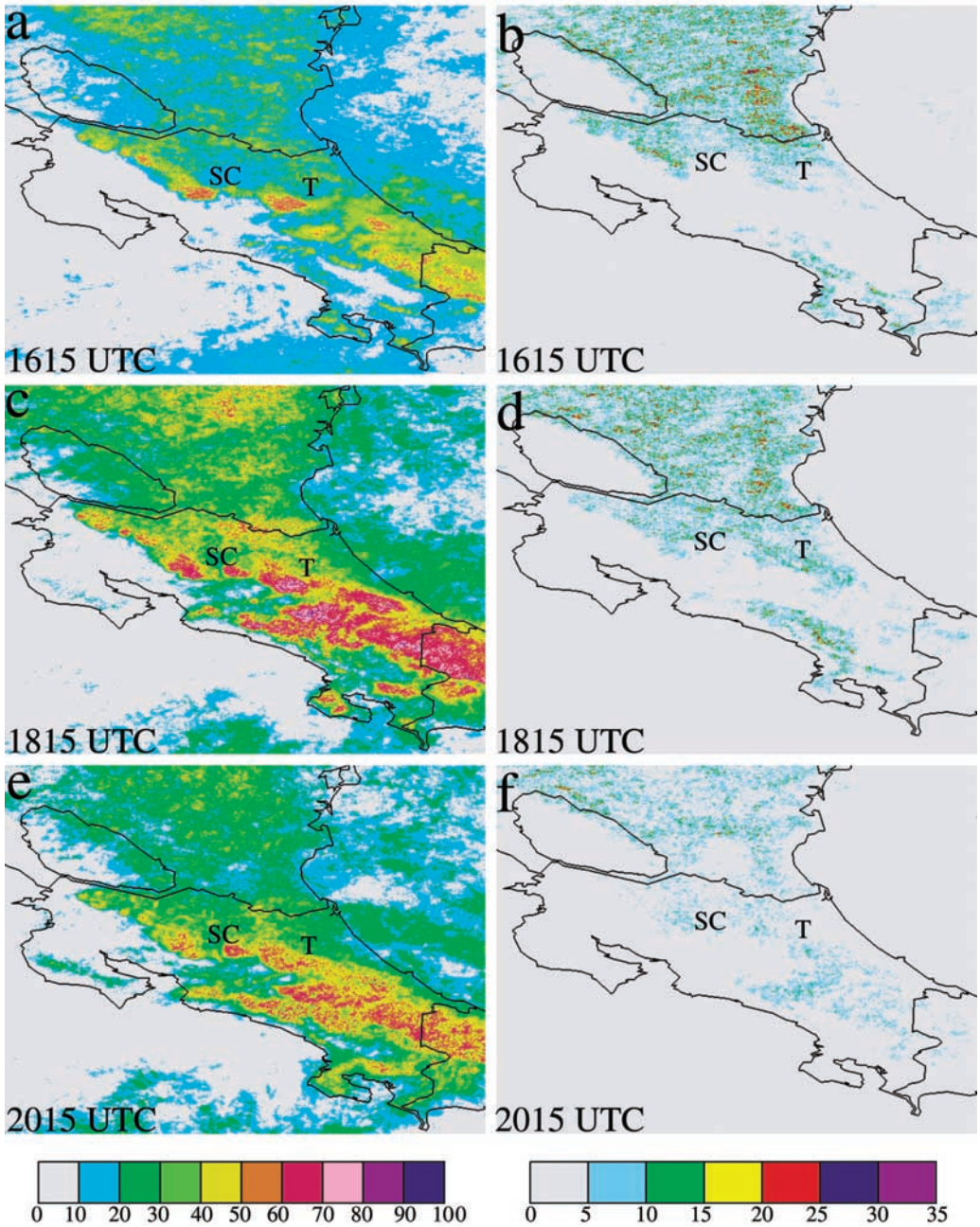

Figure 3. Percentage frequency of occurrence of total cloudiness at 1615, 1815 and 2015 UTC are shown in panels a, c and e. Percentage frequency of occurrence of cumulus clouds at these times are shown in panels b, d and f. The labeled areas in the images are San Carlos plains (SC) and Tortuguero plains (T).

months, but total cloudiness was similar. The results for February 2001 are again consistent with those for 1999 and 2000. In short, the dry season of 1999 does not seem to have been unusual.

4.2. Numerical Modeling Experiments

[26] We use the results of RAMS simulations to compare the diurnal patterns of cumulus clouds in these two environments in order to assess the effect of deforestation on cumulus cloud formation and development. In the simulations shown below it is assumed that the entire region is either pure forest or pure pasture. The issue of heterogeneous surfaces will be addressed in a subsequent paper. The results shown in Figure 4 are at 1615 UTC (1015 LST), corresponding to the time of the Landsat overpasses (Figure 2) and to the top frame of GOES images shown in Figure 3. Note that there is a strong tendency to form cloud streets in the forest simulations, as seen in the Landsat image (Figure 2b). The majority of the simulations show a transition from organized cumulus cloud streets to unorganized convection when the surface vegetation type is changed from forest (evergreen broadleaf) to pasture (short grass). This change in cloud field organization is caused by differences in sensible heat flux. Horizontal convective roll circu-

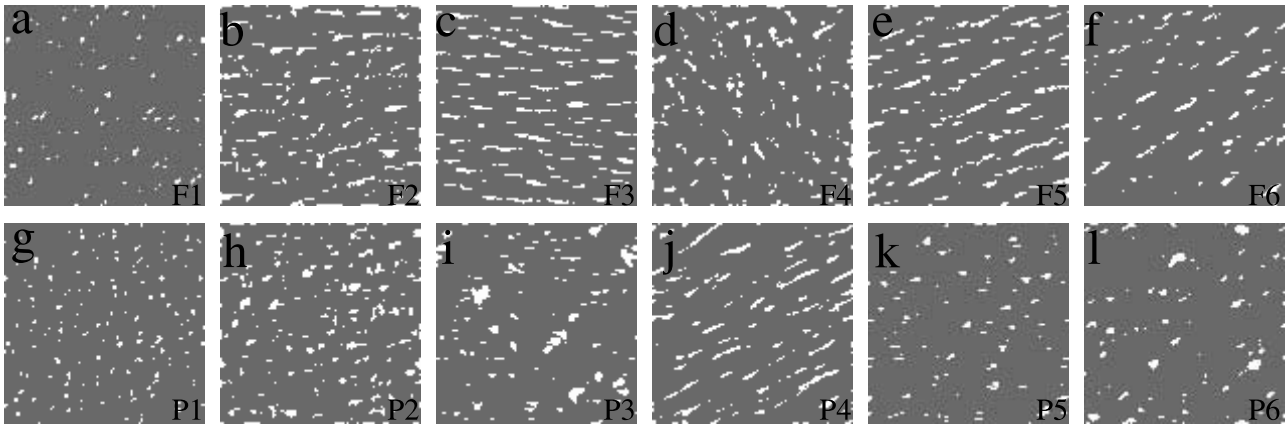

Figure 4. Simulated cloud fields at 1615 UTC from simulations F1–F6 and P1–P6 are shown in panels a–f and g–l.

lations, which are responsible for the formation of cloud streets, are caused by thermal and/or dynamic instabilities [*Weckwerth et al.*, 1997]. Typically, one utilizes non-dimensional numbers that combine the thermal and dynamic instabilities to characterize environments favorable for the formation of horizontal convective roll circulations. One such non-dimensional number is the ratio u_*/w_*. The friction velocity u_* and the free-convection scaling velocity w_* are given by:

$$u_* = \left[\overline{u'w'}_s^2 + \overline{v'w'}_s^2\right]^{\frac{1}{4}},$$

$$w_* = \left[\frac{g z_i}{\overline{\theta_v}} \overline{w'\theta'_{vs}}\right]^{\frac{1}{3}},$$

where u', v', w' and θ'_v are turbulent fluctuations of velocity components and virtual potential temperature, $\overline{u'w'}_s$ and $\overline{v'w'}_s$ are the mean surface momentum fluxes, $\overline{w'\theta'_{vs}}$ is the mean surface buoyancy flux, g is the acceleration due to gravity, z_i is the depth of convective boundary layer, and $\overline{\theta_v}$ is the mean virtual potential temperature.

[27] The u_*/w_* ratio is larger for the forest simulations compared to the pasture simulations (Table 2). *Sykes and Henn* [1989] suggested that environments with $u_*/w_* > 0.35$ are favorable for the formation of convective rolls. The u_*/w_* ratio is greater than 0.35 for the forest simulations, while for pasture simulations this ratio is less than 0.35. The surface sensible heat flux Q_H, which is given by:

$$Q_H = \rho C_p \overline{w'\theta'_v},$$

where ρ is the density of air and C_p is specific heat of air at constant pressure, is lower for forest which allows the existence of two-dimensional laminar flow necessary for the sustenance of cloud streets. However, when the surface is changed to a pasture, the enhancement in sensible heat flux makes the flow more turbulent, impeding the organization of clouds into streets.

[28] However simulation pairs F1, P1 and F4, P4 do not conform to the cloud organization followed by the other simulations (Figure 4), although the u_*/w_* ratio suggests that F1 and F4 simulations have environments favorable for the formation of cloud streets while P4 should favor unorganized convection. The expected linear organization of clouds is not present in the F1 simulation. This could be due to the inability of the model to resolve cloud streets with narrow spacing, since cloud street spacing is dependent upon boundary layer depth, which is relatively shallow for the F1 simulation. The model simulations F4 and P4 show a different pattern in which cloud organization occurs in the pasture case but not in the forest surface type. Additional study is needed to understand the reasons for this behavior.

[29] In all simulations cloud base height, averaged over the domain, shows a tendency to increase throughout the day (Figure 5). While the different soundings produce different patterns of cloud base height growth during the day, the cloud base heights in pasture simulations typically are several hundred meters higher than in the paired forest simulation. Taking the mean of the domain average of cloud base height for the six simulations (Figure 6a), cloud base height at 1600 UTC is 776 m for the forest simulations, compared to 1473 m for pasture simulations. These results are in reasonable agreement with cloud base heights determined from dry season Landsat MSS imagery using the method of *Berendes et al.* [1992]. Cloud base heights, estimated from Landsat MSS imagery for 23 March 1985 at 1615 UTC, were log normally distributed with a mean cloud base height of 736 m. Values ranged from a low of about 576 m near the coast to as high as 1099 m at the foot of the mountains.

[30] The mean difference in domain-averaged cloud base height between the six forest and pasture simulations as a function of time is shown in Figure 6b. The dashed lines show the 95% confidence intervals. The mean cloud base

Table 2. The u_*/w_* Values for Simulations F1–F6 and P1–P6 at 1615 UTC

n	Simulation Fn	Simulation Pn
1	0.93	0.26
2	0.41	0.16
3	0.93	0.26
4	0.65	0.25
5	0.83	0.31
6	0.90	0.25

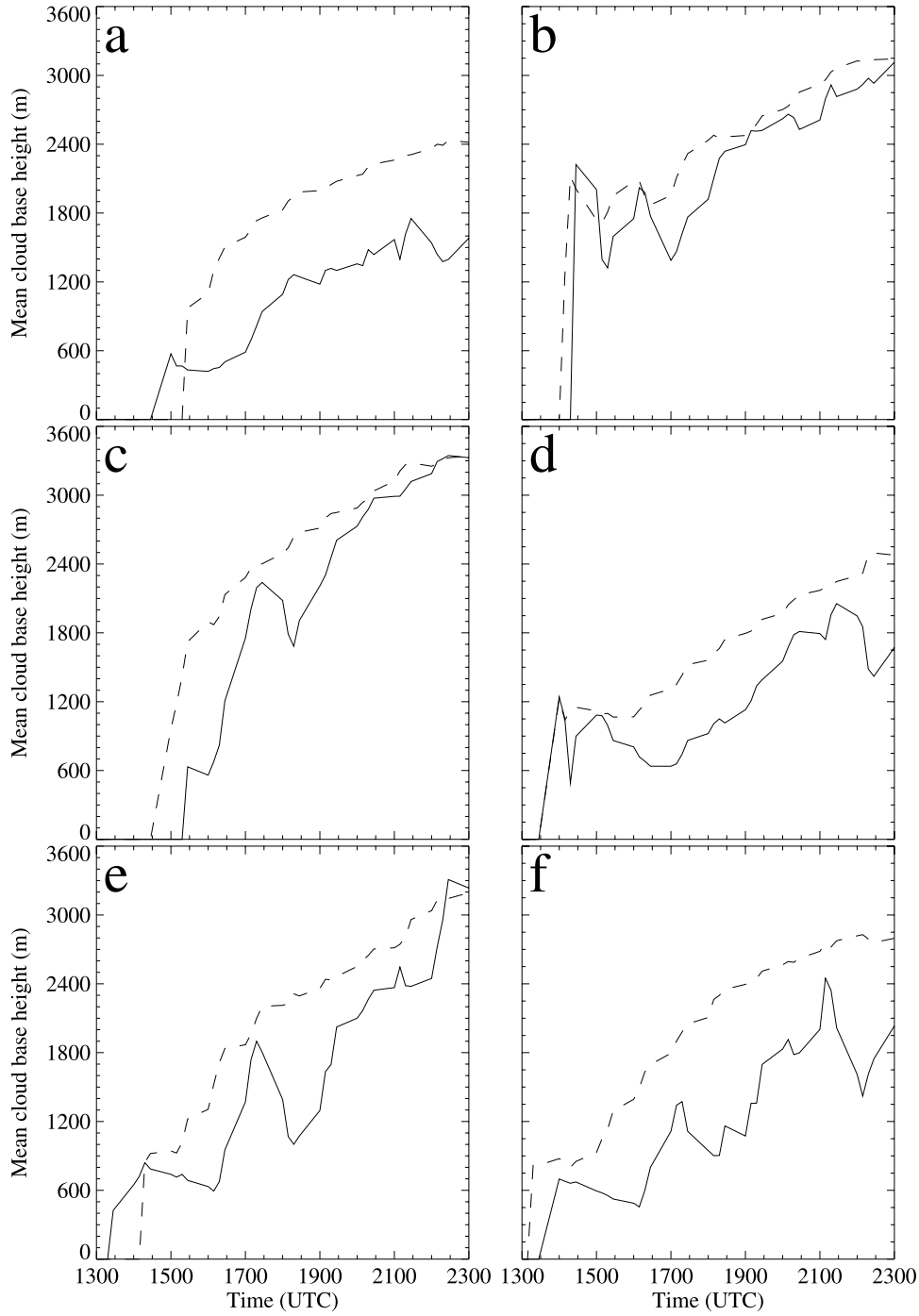

Figure 5. Comparison of diurnal variation of domain averaged cloud base height for simulations: (a) P1, F1; (b) P2, F2; (c) P3, F3; (d) P4, F4; (e) P5, F5; (f) P6, F6. The cloud base heights from forest simulations are shown as solid lines and those from pasture simulations as dashed lines.

height differences (pasture - forest) differ significantly by about 1600 UTC and then persist throughout the day. Maximum differences of about 800 m occur at about 1830 UTC.

[31] There are no significant differences in domain-averaged cloud top height for the forest and pasture simulations (not shown). However, like cloud base height, cloud top height increases rapidly in the morning, reaching mean domain-averaged values of about 2500 m at local noon. Then the increase in cloud top height slows and becomes asymptotic at a mean domain-averaged value of about 3200 m at 2000 UTC, late afternoon.

[32] Cloud thickness, the difference between cloud top height and cloud base height increases rapidly in both forest and pasture simulations until about 1600 UTC. At this time the mean domain-averaged cloud thicknesses for the six pasture simulations are about 750 m and remain at that temporarily before decreasing slowly during the remainder

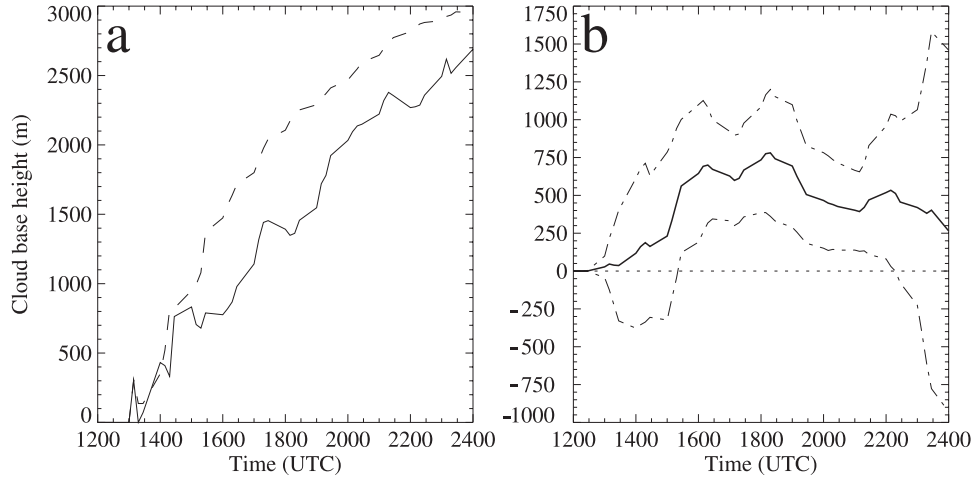

Figure 6. (a) Mean domain averaged cloud thickness for six pasture and forest simulations. The mean cloud thickness for forest simulations is shown using a solid line and for pasture using a dashed line. (b) The mean of difference in domain averaged cloud thickness between six pasture and forest simulations. The dash-dot lines show the 95% confidence curves, and the zero difference line is shown using the dashed line.

of the day. Cloud thickness increases rapidly to mean domain-averaged values of 1500 m for the forest simulations at 1700 UTC, then decreases to about 1100 m at 1800 UTC before decreasing slowly during the remainder of the day.

[33] There is considerable variation in maximum cloud coverage among the various simulations. Maximum cloud coverage for the various simulations range from a low of about 6% to a high of about 23%, but there are no consistent patterns. On the other hand, simulations showing high values of cloud cover for the forest cases similarly have high values for the pasture cases, and simulations showing low values of cloud cover for the forest cases have low values for the pasture cases. The mean cloud coverage for the six forest and pasture simulations shows a maximum of approximately 8% in the late afternoon. The mean differences in cloud cover for the forest and pasture simulations are limited to less than 2% until 2000 UTC. Then the mean cloud cover for the pasture simulations becomes about 4% larger than those for the forest simulations. This behavior is due to the fact that the maximum in mean cloud cover for the forest simulations occurs at about 1930 UTC and then cloud coverage decreases rapidly. The mean cloud cover for pasture simulations peaks at about 2100 UTC and then decreases quickly.

[34] The numerical modeling simulations of cloud fields over pasture do not suggest suppression of cumulus to the extent observed over deforested regions in GOES and Landsat imagery. The timing of initiation of convection is not significantly different for the pasture and forest simulations. However, note that the same soundings are used to prescribe the initial atmospheric structure in the simulations, whereas the actual boundary layer profile over forest and pasture will be different, with the boundary layer tending to be drier over pasture. In particular, the Convective Inhibition (CIN) for the atmospheric profile over pasture areas is expected to be higher than over forested regions. In order to resolve issues concerning the timing of convection over forested and deforested areas, specific initializing profiles over these regions are needed.

[35] On average, the cloud liquid water content is slightly higher for the six pasture simulations until 1615 UTC. After this time, the mean domain-averaged cloud liquid water content is slightly lower for the pasture cases. However the magnitude of the mean difference of cloud liquid water content is relatively small, and an analysis of the 95% confidence curves indicates that the small differences in mean cloud liquid water contents between the pasture and forest simulations are not statistically significant. The maximum mean difference during the early stages of cloud field development is about 0.16 g kg^{-2} Further, the differences between cloud liquid water contents between 1630 UTC and 2215 UTC are less than 0.1 g kg^{-1}.

[36] The mean domain-averaged liquid water path, which is liquid water content integrated as a function of height, for the forest simulations is larger than for the pasture cases after about 1600 UTC. But once again, the differences are not statistically significant at the 95% confidence level. At the first glance, the low statistical significance of differences in liquid water path between forest and pasture simulations appears inconsistent with statistically significant differences in cloud thickness. However, unlike cloud thickness, which is consistently higher for forest simulations after about 1600 UTC, the differences in liquid water content between the forest and pasture simulations are very variable. Thus, even though the mean domain averaged liquid water path for the six forest simulations is higher compared to the pasture simulations, the variances associated with the mean differences in domain averaged values for the six simulation pairs are also high. Therefore it is the large fluctuations in liquid water content that leads to the fact that the differences in liquid water path between forest and pasture simulations are not statistically significant.

[37] The mean domain-averaged sensible heat flux in the pasture simulations is significantly greater than in forest simulations (Figures 7a and 7b). The maximum mean value

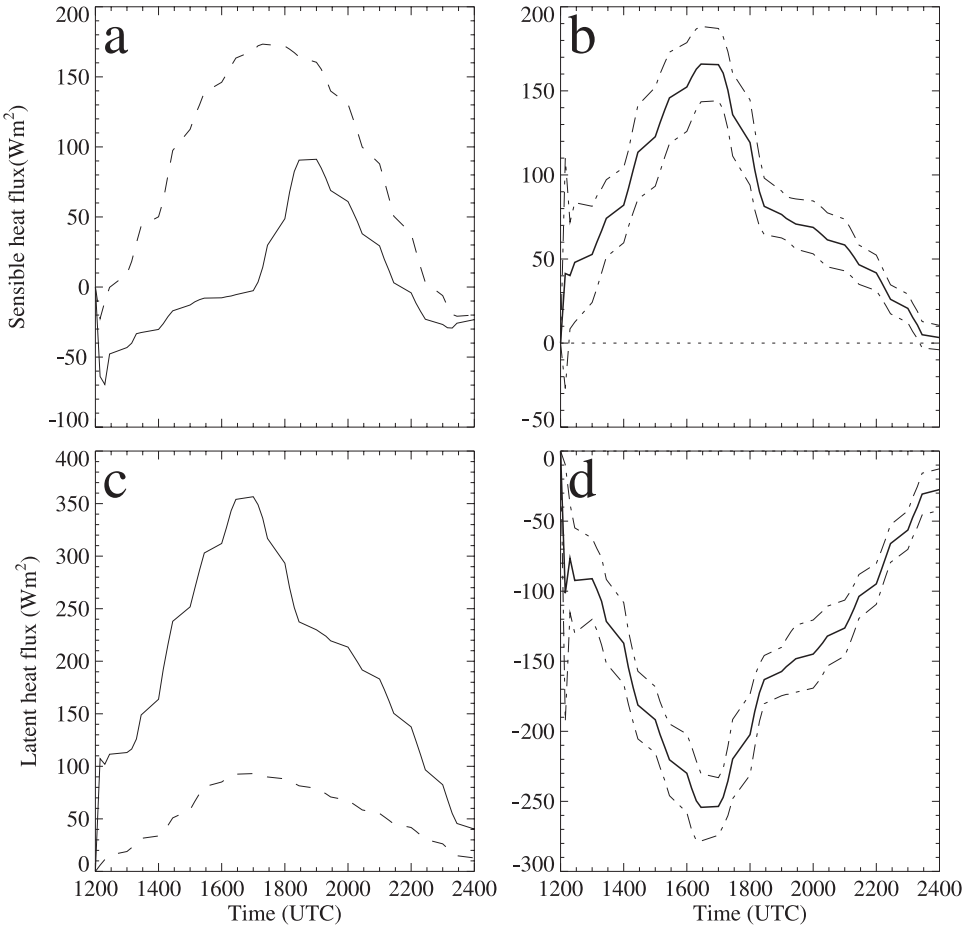

Figure 7. (a) Mean domain averaged sensible heat fluxes for six pasture and forest simulations. The sensible heat fluxes for forest simulations are shown as the solid line and for pasture as the dashed line. (b) The mean of differences in domain averaged sensible heat fluxes between six pasture and forest simulations. (c) Mean domain averaged latent heat flux for six pasture and forest simulations. The mean latent heat flux for forest simulations is shown as the solid line and for pasture as the dashed line. (d) The mean of difference in domain averaged latent heat flux between six pasture and forest simulations. The dash dot lines in Figures 7b and 7d show the 95% confidence curves, and the zero difference line is shown as the dashed line in Figure 7b.

of sensible heat flux for the pasture simulations is 173 Wm^{-2} at 1730 UTC, compared to a maximum value of 91 Wm^{-2} at 1900 UTC for the forest simulations. Note that the mean sensible heat flux for the pasture simulations is positive for the time period of 1300 to 2245 UTC, whereas it is positive for the forest simulations only between 1715 and 2145 UTC. The maximum mean difference in sensible heat flux between pasture and forest simulations is 171 Wm^{-2} at 1700 UTC (Figure 7b).

[38] The mean domain-averaged latent heat fluxes also differ significantly between pasture and forest simulations (Figure 7c). The mean latent heat fluxes for both sets of simulations peaks at 1700 UTC, at 356 Wm^{-2} for the forest simulations and 93 Wm^{-2} for the pasture simulations. The largest difference in mean latent heat fluxes is 263 Wm^{-2} at 1700 UTC (Figure 7d).

[39] Figure 8a shows mean domain-averaged values of surface temperature as a function of time for the forest and pasture simulations. The pasture landscapes have significantly higher surface temperatures than forests throughout the simulations (Figures 8a and 8b). The pattern of diurnal variation of surface air temperature is similar for pastures and forests, but the amplitudes are different. The pastures achieve a maximum mean surface air temperature of 31.5°C at 2130 UTC, while the forests achieve a maximum value of 27.9°C at 2100 UTC. The mean differences in surface air temperature increase from approximately 1.5°C at 1300 UTC to a maximum of 4.1°C at 1745 UTC. After 1715 UTC the difference in surface air temperature remains relatively constant through the remainder of the simulation period.

[40] The mean domain-averaged surface dewpoint temperatures for pasture simulations are lower than those of forest simulations throughout the day (Figures 9a and 9b). Forest mean surface dewpoint temperatures increase early in the day, reaching a maximum value of 24.1°C at 1645 UTC, then decrease slightly but remaining relatively constant for the remainder of the day. In contrast, the pasture surface dewpoint temperatures are about 22°C early in the simulations, but then steadily decrease for most of the remainder

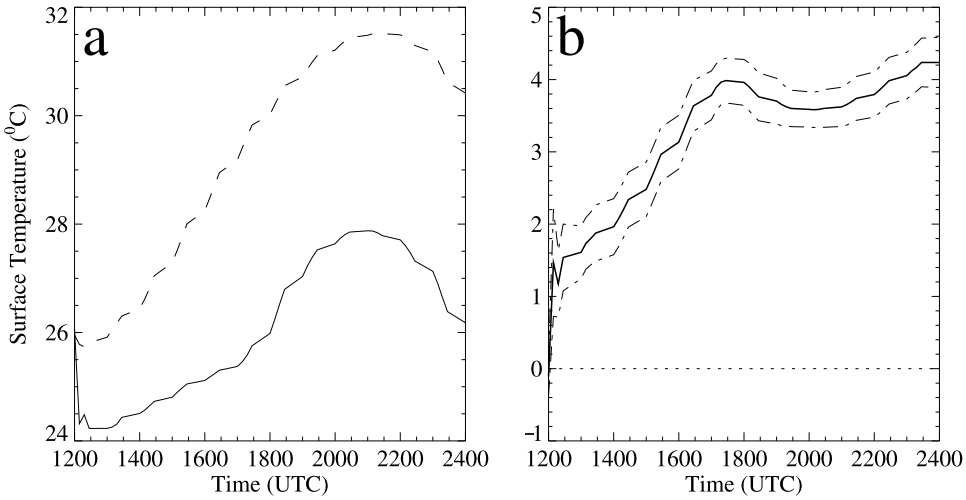

Figure 8. (a) Mean domain averaged surface air temperature for six pasture and forest simulations. The mean surface air temperature for forest simulations is shown using solid line and for pasture using dashed line. (b) The mean of difference in domain averaged surface air temperature between six pasture and forest simulations. The dash dot lines in show the 95% confidence curves and the zero difference line is shown using dashed line.

of the day, with minimum values of about 16.5°C at 2200 UTC. The mean difference in surface dewpoint temperature changes steadily from a value of about −1°C (i.e., pasture - forest) at 1200 UTC to a value of −5.8°C at 1815 UTC.

5. Conclusions

[41] The impact of tropical deforestation on local and regional climates has been a matter of growing concern [*Shukla et al.*, 1990; *Gash and Nobre*, 1997], raised initially by well-known differences in microclimates and local energy budgets between forests and adjacent grasslands and croplands [*Geiger*, 1971]. The results we report here suggest that tropical deforestation and associated land use changes can alter characteristics of the overlying atmosphere in ways that influence dry season cloud formation in settings that have serious climatic implications for adjacent montane environments.

[42] The frequency of occurrence of dry season cumulus cloud fields over northern Costa Rica, derived from GOES 8 imagery, is spatially associated with the pattern of lowland deforestation. Late morning cumulus cloudiness was suppressed over deforested areas. Further, the degree of suppression varies with the amount of deforestation, the suppression being strongest for the most thoroughly deforested area. This presumably occurs because cumulus cloud

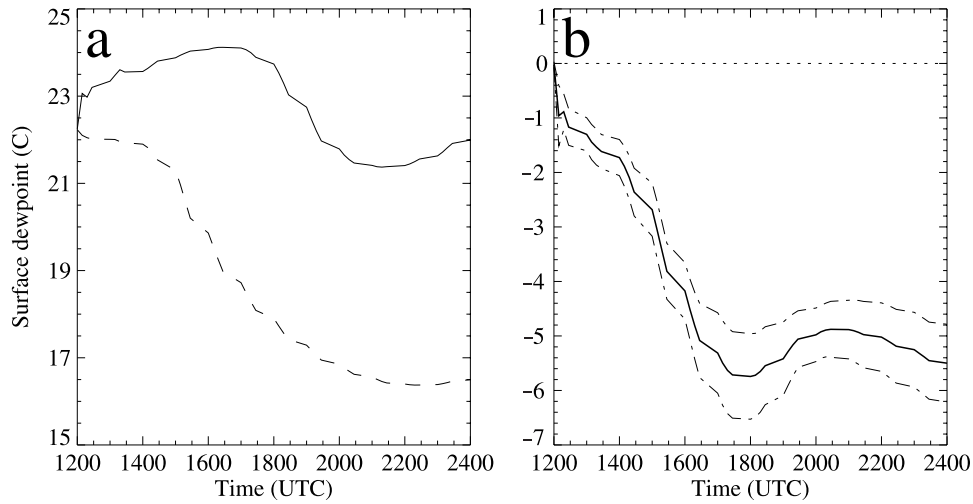

Figure 9. (a) Mean domain averaged surface air dewpoint temperature for six pasture and forest simulations. The mean surface air dewpoint temperature for forest simulations is shown using solid line and for pasture using dashed line. (b) The mean of difference in domain averaged surface air dewpoint temperature between six pasture and forest simulations. The dash dot lines show the 95% confidence curves and the zero difference.

formation is strongly influenced by the surface through modification of the surface energy budget It should be noted that the current observations of suppression of cumulus clouds over deforested areas are in contradiction to prior studies showing enhanced cumulus cloudiness over deforested areas [*Rabin et al.*, 1990; *Lyons et al.*, 1993; *Cutrim et al.*, 1995]. However note that the atmospheric conditions in this study are significantly different compared to those considered in these prior studies.

[43] The RAMS simulations suggest that reduced cloudiness over deforested areas in the dry season is due to reduced latent heat fluxes and concomitantly enhanced sensible heat fluxes in comparison to the originally forested landscape. Surface air temperature is consistently higher for pasture, and surface dewpoint temperature is higher for forest in paired simulations. In the RAMS simulations warmer and drier air is found over pastures than over forests, resulting in the changes in cloud formation.

[44] The RAMS simulations show that mean cloud base height for the pasture simulations are consistently and significantly higher than in the paired forest simulations. As a result clouds are significantly thicker over the forested landscape, although differences in cloud top heights between the pasture and forest simulations are not statistically significant.

[45] The simulation results from the present study are in general agreement with those of a large eddy simulation study of the sensitivity of cumulus clouds to soil moisture over the Atmospheric Radiation Measurement (ARM) site in Oklahoma [*Golaz et al.*, 2002]. They also found increased cloud base heights and decreased cloud thickness associated with decreased soil moisture, while cloud top heights and liquid water contents remain relatively unchanged [*Golaz et al.*, 2002]. In addition they found lower mean liquid water paths associated with decreased soil moisture, but we report here only statistically insignificantly lower values of mean liquid water path for the six pasture simulations compared to their forest counterparts.

[46] Although the simulations in this study are topographically unrealistic in that they utilize a perfectly flat landscape, their correspondence with Landsat and GOES observations suggests that this lack of realism does not obscure the importance or applicability of the results. In northern Costa Rica, as in many parts of the tropics, dry season trade winds blow across lowlands before being forced to rise over mountains, forming orographic cloud decks that define the character and distribution of tropical montane cloud forests [*Clark et al.*, 2000].

[47] In these cloud forests dry season water input is almost entirely a matter of the direct deposition of cloud droplets and mist as the orographic clouds move through the forest. Since the air masses in lowland regions are ultimately responsible for the formation of orographic clouds, modification of the lowland cloudbanks crucial to cloud forests such as that at Monteverde in northern Costa Rica. After all, the primary difference between free convective cumulus and a stratocumulus orographic bank is the lifting mechanism. Processes affecting the boundary layer will influence formation and development of both cloud types. The warming and drying of boundary layer air in the lowland regions could thus increase the cloud base heights of the orographic cloudbanks.

[48] Regional climate change with associated serious ecological implications in the Monteverde cloud forest has been documented recently [*Still et al.*, 1999; *Pounds et al.*, 1999]. Since the mid-1970s there has been a reduction in the dry season days with wind-blown mist, the major source of dry season moisture. The reduction of dry season moisture may have contributed to anuran population crashes observed in this region [*Pounds et al.*, 1999]. It has been suggested that the reduction in dry season moisture input due to increased cloud base heights results from elevated sea surface temperatures [*Still et al.*, 1999; *Pounds et al.*, 1999]. In this study we provide the alternative hypothesis that deforestation alters surface energy budget in ways that influence the development of Costa Rican dry season cumulus cloud fields and orographic cloud fields. Further investigation is needed to examine this hypothesis.

[49] The elevation of cloud base height resulting from lowland deforestation could have serious implications for tropical montane cloud forests throughout the tropics. Local hydrological changes resulting from deforestation have already been documented [*Meher-Homji*, 1991], and shifts in regional climate in tropical montane settings may have serious local ecological impacts [*Pounds et al.*, 1999]. Systematic measurements of cloud base heights and field experiments to observe the atmospheric and land surface variables over forested and deforested areas are required to better understand the regional climate changes occurring in coupled lowland and montane regions in the tropics.

[50] In summary: (1) Satellite imagery shows a pattern of suppression of cumulus cloud formation over deforested lowland regions of northern Costa Rica. The degree of suppression appears to be associated with the extent of deforestation. Cloud suppression over deforested regions is strongest during the month of March, the peak of the dry season. Satellite imagery also shows that the deforested regions show development of clouds during the later hours of the day. (2) Paired RAMS simulations of tropical lowland pasture and forest landscapes show enhanced sensible heat fluxes and reduced latent heat fluxes over pasture compared to forest. This results in drier and warmer air over pasture surfaces. (3) RAMS numerical modeling experiments show statistically significant differences in cloud base height and cloud thickness between cloud fields forming over forest and pasture surfaces. On average the clouds have lower base heights and are thicker over forest surfaces. Differences in cloud top heights between forest and pasture simulations are not statistically different. (4) For the same initial atmospheric conditions, differences in cloud cover between forest and pasture simulations are only statistically significant during the later hours of the day. The pasture and forest simulations do not differ significantly in cloud water mixing ratio and cloud liquid water paths. (5) Modification of boundary layer air over deforested tropical lowland regions could lead to elevation of the base of orographic cloudbanks in downwind mountain ranges.

[51] **Acknowledgments.** This research was supported by National Aeronautics and Space Administration (NASA) CERES contract NAS5-31718, NASA ASTER contract NAS1-98131, NASA grant NAG5-11941, and National Science Foundation grant ATM-0128924. The authors are thankful to Jean-Christophe Golaz, Mark Hjemfelt, and Tammy Weckwerth for advice and helpful comments. The GOES 8 data was acquired by GOES ground station at Global Hydrology and Climate Center, Huntsville,

Alabama. We are thankful for the helpful comments and suggestions of the reviewers.

References

Anthes, R., Enhancement of convective precipitation by mesoscale variations in vegetative covering in semiarid regions, *J. Clim. Appl. Meteorol.*, *23*, 541–554, 1984.

Avissar, R., and Y. Liu, Three-dimensional numerical study of shallow convective clouds and precipitation induced by land surface forcing, *J. Geophys. Res.*, *101*, 7499–7518, 1996.

Avissar, R., and R. A. Pielke, A parameterization of heterogeneous land surfaces for atmospheric models and its impact on regional meteorology, *Mon Weather Rev.*, *117*, 2113–2136, 1989.

Avissar, R., and T. Schmidt, An evaluation of scale at which ground-surface heat flux patchiness affects the convective boundary layer using large-eddy simulations, *J. Atmos. Sci.*, *55*, 2666–2689, 1998.

Bastable, H. G., W. J. Shuttleworth, R. L. G. Dallarosa, G. Fisch, and C. A. Nobre, Observations of climate, albedo and surface radiation over cleared and undisturbed Amazonian forest, *Int. J. Clim.*, *13*, 783–796, 1993.

Berendes, T., S. K. Sengupta, R. M. Welch, B. A. Wielicki, and M. Navar, Cumulus cloud base height estimation from high spatial resolution Landsat data: A Hough transform approach, *IEEE Trans. Geosci. Remote Sens.*, *30*(3), 430–443, 1992.

Bluestein, H. B., *Synoptic-Dynamic Meteorology in Midlatitudes*, vol. 2, *Observations and Theory of Weather Systems*, 594 pp., Oxford Univ. Press, New York, 1992.

Bruinjzeel, L. A., and J. Proctor, *Tropical Montane Cloud Forests*, edited by L. S. Hamilton, J. O. Juvik, and F. N. Scatena, pp. 38–78, Springer-Verlag, New York, 1995.

Bryant, N. A., L. F. Johnson, A. J. Brazel, R. C. Balling, C. F. Hutchinson, and L. R. Beck, Measuring the effect of overgrazing in the Sonoran Desert, *Clim. Change*, *17*, 234–264, 1990.

Chen, C., and W. R. Cotton, A one-dimensional simulation of the stratocumulus-capped mixed layer, *Boundary Layer Meteorol.*, *25*, 289–321, 1983.

Chen, F., and R. Avissar, Impact of land-surface moisture variability on local shallow convective cumulus and precipitation in large-scale models, *J. Appl. Meteorol.*, *33*, 1382–1394, 1994.

Clark, K. L., R. O. Lawton, and P. R. Butler, *Physical Environment*, *Monteverde: Ecology and Conservation of a Tropical Cloud Forest*, edited by N. M. Nadkarni and N. T. Wheelwright, chap. 3, pp. 15–38, Oxford Univ. Press, New York, 2000.

Cutrim, E. D., W. Martin, and R. Rabin, Enhancement of cumulus clouds over deforested lands in Amazonia, *Bull. Am. Meteorol. Soc.*, *76*, 1801–1805, 1995.

Dietrich, W. E., D. M. Windsor, and T. Dunne, *The Ecology of a Tropical Forest*, edited by E. G. Leigh, A. S. Rand, and D. M. Windsor, pp. 21–46, Smithsonian Inst. Press, Washington, D. C., 1982.

Emori, S., Interaction of cumulus convection with soil moisture distribution: An idealized simulation, *J. Geophys. Res.*, *103*, 8873–8884, 1998.

Gash, J. H. C., and C. A. Nobre, Climatic effect of Amazonian deforestation: Some results from ABRACOS, *Bull. Am. Meteorol. Soc.*, *78*, 823–830, 1997.

Geiger, G., *Climate Near the Ground*, 611 pp., Harvard Univ. Press, Cambridge, Mass., 1971.

Gibson, H. M., and T. H. Vonder Haar, Cloud and convection frequencies over the southeast United States as related to small-scale geographic features, *Mon. Weather Rev.*, *118*, 2215–2227, 1990.

Golaz, J.-C., H. Jiang, and W. R. Cotton, A large-eddy simulation study of cumulus clouds over land and sensitivity to soil moisture, *Atmos. Res.*, *59*, 373–392, 2002.

Lyons, T. J., P. Schwerdtfeger, J. M. Hacker, I. J. Foster, R. C. G. Smith, and H. Xinmei, Land-atmosphere interaction in a semiarid region: The bunny fence experiment, *Bull. Am. Meteorol. Soc.*, *74*, 1327–1334, 1993.

Meher-Homji, V. M., Probable impact of deforestation on hydrological processes, *Clim. Change*, *19*, 163–173, 1991.

Nair, U. S., Climatic impact of lowland deforestation on tropical montane cloud forests in Costa Rica, 122 pp., Ph.D. dissertation, Dep. of Atmos. Sci., Colo. State Univ., Fort Collins, 2002.

Nair, U. S., J. A. Rushing, R. Ramachandran, K. S. Kuo, R. M. Welch, and S. J. Graves, Detection of cumulus cloud fields in satellite imagery, in *Earth Observing Systems IV*, edited by W. L. Barnes, *Proc. SPIE, 3750*, 345–355, 1999.

Ookouchi, Y., M. Segal, R. C. Kessler, and R. A. Pielke, Evaluation of soil moisture effects on generation and modification of mesoscale circulations, *Mon. Weather Rev.*, *112*, 2281–2292, 1984.

Otterman, J., Baring high-albedo soils by overgrazing: A hypothesized desertification mechanism, *Science*, *86*, 531–533, 1974.

Otterman, J., A. Manes, S. Rubin, P. Alpert, and D. O'C. Starr, An increase of early rains in southern Israel following land-use change?, *Boundary Layer Meteorol.*, *53*, 333–351, 1990.

Pielke, R. A., A three-dimensional numerical model of the sea breezes over south Florida, *Mon. Weather Rev.*, *102*, 115–139, 1974.

Pielke, R. A., Sr., Influence of the spatial distribution of vegetation and soils on the prediction of cumulus convective rainfall, *Rev. Geophys.*, *39*, 151–178, 2001.

Pielke, R. A., and X. Zeng, Influence of severe storm development of irrigated land, *Natl. Weather Dig.*, *14*, 16–17, 1989.

Pielke, R. A., et al., A comprehensive meteorological modeling system: RAMS, *Meteorol. Atmos. Phys.*, *49*, 69–91, 1992.

Pounds, A. J., M. P. L. Fogden, and J. H. Campbell, Biological response to climate change on tropical mountain, *Nature*, *389*, 611–614, 1999.

Rabin, R. M., and D. W. Martin, Satellite observations of shallow cumulus coverage over the central United States: An exploration of landuse impact on cloud cover, *J. Geophys. Res.*, *101*, 7149–7155, 1996.

Rabin, R. M., S. Stadler, P. J. Wetzel, D. J. Stensrud, and M. Gregory, Observed effect of landscape variability on convective clouds, *Bull. Am. Meteorol. Soc.*, *71*, 272–280, 1990.

Sader, S. A., and A. T. Joyce, Deforestation rates and trends in Costa Rica, 1940 to 1983, *Biotropica*, *20*, 11–19, 1988.

Sagan, C., O. B. Toon, and J. B. Pollack, Anthropogenic albedo changes an the Earth's climate, *Science*, *206*, 1363–1368, 1979.

Schwartz, M. D., and T. R. Karl, Spring phenology: Nature's experiment to detect the effect of "green-up" on surface maximum temperatures, *Mon. Weather Rev.*, *114*, 883–890, 1990.

Segal, M., R. Avissar, M. C. McCumber, and R. A. Pielke, Evaluation of vegetation effects on the generation and modification of mesoscale circulations, *J. Atmos. Sci.*, *45*, 2268–2292, 1988.

Segal, M., R. W. Arrit, J. Shen, C. Anderson, and M. Leuthold, On the clearing of cumulus clouds downwind from the lakes, *Mon. Weather Rev.*, *125*, 639–646, 1997.

Shukla, J., C. Nobre, and P. Sellers, Amazon deforestation and climate change, *Science*, *247*, 1322–1325, 1990.

Still, C. J., P. N. Foster, and S. H. Schneider, Simulating the effects of climate change on tropical montane cloud forests, *Nature*, *389*, 608–610, 1999.

Sud, Y. C., W. C. Chao, and G. K. Walker, Dependence of rainfall on vegetation: theoretical considerations, simulation experiments, observations, and inferences from simulated atmospheric soundings, *J. Arid Environ.*, *25*, 5–18, 1993.

Sykes, R. I., and D. S. Henn, Large-eddy simulation of turbulent sheared convection, *J. Atmos. Sci.*, *35*, 25–39, 1989.

Tremback, C. J., and R. Kessler, A surface temperature and moisture parameterization for use in mesoscale numerical models, in *Proceedings of the 7thAMS Conference on Numerical Weather Prediction, June 17–20. Montreal, Quebec, Canada*, pp. 355–358, Am. Meteorol. Soc., Boston, Mass., 1985.

Weckwerth, T. M., J. W. Wilson, R. M. Wakimoto, and N. A. Crook, Horizontal convective rolls: Determining the environmental conditions supporting their existence and characteristics, *Mon. Weather Rev.*, *125*, 505–526, 1997.

Wetzel, P. J., S. Argentini, and A. Boone, Role of land surface in controlling daytime cloud amount: Two case studies in GCIP-SW area, *J. Geophys. Res.*, *101*, 7359–7370, 1996.

Wheelwright, N. T., Conservation biology, in *Monteverde: Ecology and Conservation of a Tropical Cloud Forest*, edited by N. M. Nadkarni and N. T. Wheelwright, chap. 12, pp. 419–456, Oxford Univ. Press, New York, 2000.

Wright, I. R., J. H. C. Gash, H. R. da Rocha, W. J. Shuttleworth, C. A. Nobre, G. T. M. Maitelli, C. A. G. P. Zamparoni, and P. R. A. Carvalho, Dry season micrometeorology of central Amazonian ranchland, *Q. J. R. Meteorol. Soc.*, *118*, 1083–1099, 1992.

R. O. Lawton, Department of Biological Sciences, University of Alabama in Huntsville, Huntsville, AL 35899, USA.

U. S. Nair and R. M. Welch, Department of Atmospheric Science, National Space Science and Technology Center, University of Alabama in Huntsville, 320 Sparkman Drive, Huntsville, AL 35806, USA. (nair@nsstc.uah.edu)

R. A. Pielke Sr., Department of Atmospheric Science, Colorado State University, Fort Collins, CO 80523-1371, USA.